

# We are IntechOpen, the world's leading publisher of Open Access books Built by scientists, for scientists

6,900

Open access books available

186,000

International authors and editors

200M

Downloads

Our authors are among the

154

Countries delivered to

TOP 1%

most cited scientists

12.2%

Contributors from top 500 universities



WEB OF SCIENCE™

Selection of our books indexed in the Book Citation Index  
in Web of Science™ Core Collection (BKCI)

Interested in publishing with us?  
Contact [book.department@intechopen.com](mailto:book.department@intechopen.com)

Numbers displayed above are based on latest data collected.  
For more information visit [www.intechopen.com](http://www.intechopen.com)



# Extracting Individual Properties from Global Behaviour: First-order Reversal Curve Method Applied to Magnetic Nanowire Arrays

Fanny Béron<sup>1</sup>, Louis-Philippe Carignan<sup>2</sup>, David Ménard<sup>2</sup> and Arthur Yelon<sup>2</sup>

<sup>1</sup>*Universidade Estadual de Campinas (UNICAMP),*

<sup>2</sup>*École Polytechnique de Montréal*

<sup>1</sup>*Brazil*

<sup>2</sup>*Canada*

## 1. Introduction

The behaviour of a group cannot be simply reduced to the sum of the behaviour of individuals (Le Bon, 1895). Examples abound in nature: school of fish or swarms of insect act like a single individual, but with emergent properties, i.e. properties which none of the individuals in the group possess, but which appear when these individuals are grouped into a system. A key element characterising a crowd is that the individuals should know that they are part of an ensemble (Le Bon, 1895). In other words, there must be interactions between them, on a short or long range. Otherwise they only constitute a system of several isolated individuals without emergent properties. Whatever the system, it is usually much easier to access its global behaviour, compared to the behaviour of individuals and their method of communication. However, the understanding of the global behaviour, in order to be able to control it subsequently, necessarily requires the knowledge of individual behaviour and of their interactions.

According to these criteria, the magnetic behaviour of structures composed of magnetic entities embedded in a non-magnetic matrix must be considered as a crowd: entities "talking" to each other via exchange or dipolar interactions depending upon the distance that separates them. Therefore, the behaviour of the global (or collective) structure may differ from that of the local (or individual) entities. This difference will be accentuated in the presence of non-uniformity (geometric, structural, etc.) of the entities. To access the magnetostatic properties of a system (coercivity, remanence, interactions, etc.), one usually uses a magnetometer to measure the major hysteresis curve. It is possible to use the same experimental setup to obtain the local magnetostatic properties of the system, by measuring multiple minor hysteresis curves, called first-order reversal curves (FORC) (Mayergoyz, 1985). This technique can be particularly efficient and powerful in the case of highly interacting systems, like ferromagnetic nanowire arrays (Fig. 1). The large dipolar interaction field between the wires, associated with small interwire distance, strongly affects the overall array behaviour. Array properties (high anisotropy, resonance frequency in the gigahertz, etc.) make them promising candidates for high frequency devices (Saib et al., 2005), high-density magnetic memories (Almawlawi et al., 1991; Ross, 2001) and sensors (Lindeberg &

Source: Electrodeposited Nanowires and Their Applications, Book edited by: Nicoleta Lupu, ISBN 978-953-7619-88-6, pp. 228, February 2010, INTECH, Croatia, downloaded from SCIYO.COM

Hjort, 2003). Moreover, with a multilayer structure (i.e. alternation of magnetic and non-magnetic nanodiscs), controlling the ratio between the magnetic and non-magnetic nanodiscs provides easy control of the effective anisotropy of the array (Tang et al., 2007; Carignan et al., 2007). This possibility makes the multilayer nanowire array particularly interesting for high frequency devices (Ye et al., 2007), especially circulators (Saib et al., 2001), although the initial goal of using multilayer nanowires was to obtain giant magnetoresistance devices (Blondel et al., 1994, Piroux et al., 1994; Piroux et al., 2007).

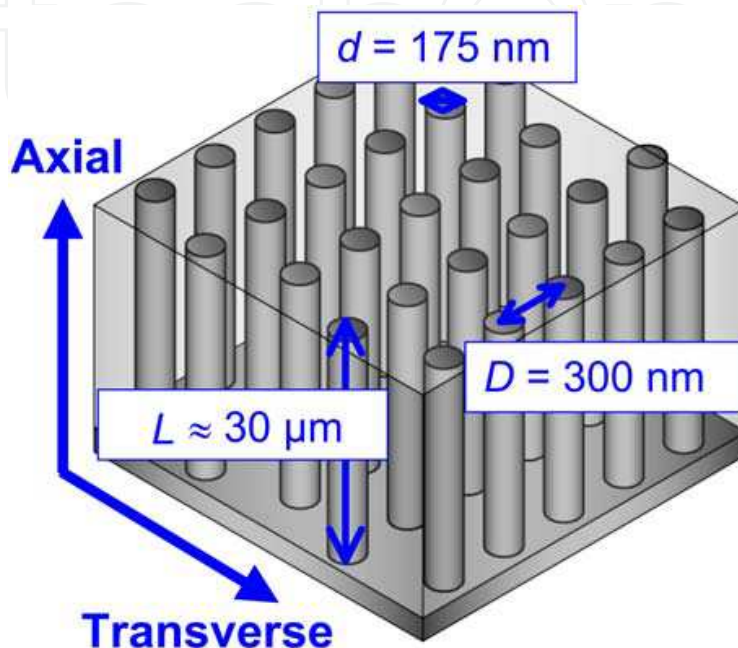


Fig. 1. Schematic of a ferromagnetic nanowire array. The geometric dimensions (diameter  $d$ , interwire distance  $D$  and length  $L$ ) are indicated, as are the two principal directions (axial and transverse) for the application of an external magnetic field.

Despite the advantages of the FORC method for nanowire array characterisation, few studies exist on the subject (Spinu et al., 2004; Béron et al., 2006; Lavín et al., 2008; Peixoto & Cornejo, 2008; Béron et al., 2008b). This is mainly due to the lack of interpretative models suitable for highly interacting systems. This confines the analysis of the FORC result, which graphically represents the magnetisation reversal, to qualitative conclusions. This problem motivated the elaboration of the physical analysis model (Béron et al., 2008a), which is based on physically meaningful hypotheses. It is therefore possible to extract the intensity and spatial distribution of the interaction field at saturation, the coercivity distribution of individual nanowires (Béron et al., 2008b) and a quantitative evaluation of the overall magnetic anisotropy (Béron et al., 2007). In addition, insights about the magnetisation reversal mechanism can also be obtained. Here, we demonstrate the utility of FORC characterisation of nanowire arrays by showing how to extract these local properties from a global measurement. The versatility of the FORC method is demonstrated by presenting experimental examples of nanowire arrays with different saturation magnetisations ( $\text{Ni} = 490 \text{ emu/cm}^3$ ,  $\text{Co}_{94}\text{Fe}_5\text{B}_1 = 1500 \text{ emu/cm}^3$ ), structures (uniform or multilayer) and applied field directions (parallel or perpendicular to the nanowire axis).

For systems such as arrays of nanoparticles with high dispersion of such properties as particle size, spacing and geometry, it may be more difficult to analyse the effects of these

parameters, and to develop the kind of physical models described here. For systems such as sheets of transformer steel, it may even be difficult to identify physically meaningful objects whose properties and interactions may be modelled. However, we believe that the FORC method is sufficiently powerful, and the physical modelling approach presented here is sufficiently promising, that effort in this direction is likely to be rewarded.

## 2. First-order reversal curve (FORC) method

Application of the FORC method requires that the system exhibits hysteretic behaviour. A phenomenon is called hysteretic when, for a given value of input, there exist several possible output values. The principal consequence is the division into two paths between the saturation points, depending on the direction of variation of the input. The set of the two branches is called hysteresis cycle or major hysteresis curve, while the term hysteresis area refers to the interval between the saturation points, i.e. where the two paths are not superposed (Fig. 2). The remanence represents the state for a null input, while the coercivity is the input value needed for the system to give a null output. Finally, the slope of the hysteresis curve is called susceptibility ( $\chi$ ). The easy axis of a system refers to the easiest direction to magnetise, for which the energy is a minimum in the absence of an input. This implies the presence of some anisotropy in the system (shape, crystalline, surface, etc.)

From a mathematical point of view, a hysteretic phenomenon can be described as a transducer for which the input-output relationship has multiple branches, a branch transition occurring for each applied extreme input value. A hysteresis mathematical model thus needs to keep in memory the previous extreme applied input values (Mayergoyz, 1985).

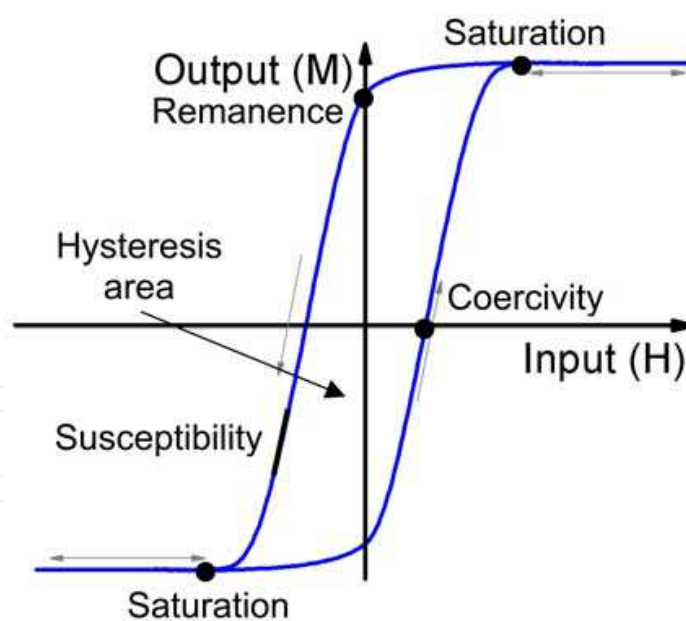


Fig. 2. Characteristics of a hysteresis curve.

The nature of the physical phenomena exhibiting a hysteresis is exceedingly diverse: magnetic, mechanical, optical, etc. However, because of its mathematical nature, the following model and the conclusions derived from it remain valid regardless of the physical phenomenon. One just needs to adjust the input and output variables with the correct parameters, for example, the applied magnetic field and the magnetisation in case of magnetic materials, or the applied tension and the deformation generated for a plastic material.

### 2.1 Measurement and calculations

The FORC method was based, at its origin, on the classical Preisach model (Preisach, 1938), a mathematical model where hysteresis can be modelled as a set of elementary processes, or operators, called hysterons and characterized by two parameters,  $H_c$  and  $H_u$  (Fig. 3). It is important to note that these hysterons do not necessarily have a physical significance, and so, will subsequently be called “mathematical hysterons” (Mayergoyz, 1985). Indeed, when applying the FORC method to a physical system, one does not need to use the classical Preisach model to interpret the result. Several different approaches are possible, either based on physical hypothesis (ex. physical analysis model, Béron et al., 2008a) or on mathematical distributions (ex. moving Preisach model, Della Torre, 1966).

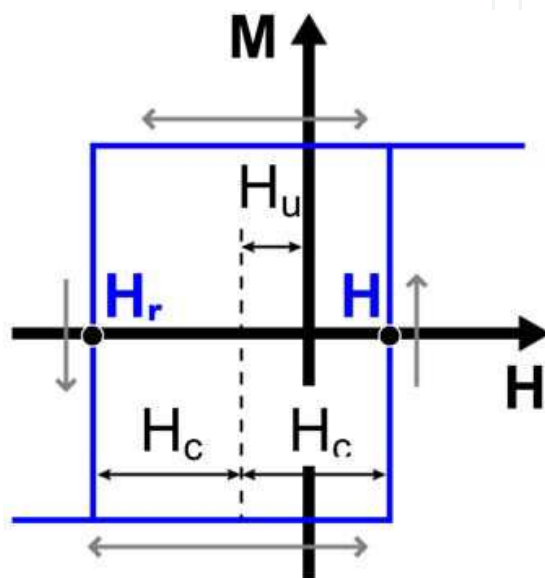


Fig. 3. Mathematical hysteron from the classical Preisach model. The magnetisation switches down, abruptly, at  $H_r = -(H_c + H_u)$ , and switches back up for a certain  $H = (H_c - H_u)$  value. It is completely described by the  $H_c$  and  $H_u$  parameters, which respectively represent the coercivity and the bias field of the mathematical hysteron.

The goal of any FORC measurements is to retrieve the  $H_c$  and  $H_u$  parameters of each mathematical hysteron of the system. To achieve this, the system is first positively saturated, in order to put all the magnetisation of the hysterons in the “up” position. The input variable (in our case, the external applied field  $H$ ) is then lowered until a point called reversal field ( $H_r$ ), which switches “down” the magnetisation of some hysterons, depending upon their  $H_c$  and  $H_u$  parameters. Then, the field  $H$  is increased again and the magnetisation  $M$  is measured. The difference of magnetisation between the applied field and the reversal field is directly proportional to the amount of hysterons that switched back “up”. This kind of minor hysteresis curve is called first-order reversal curve. The information about all hysterons in the system, the FORC distribution  $\rho_{FORC}$ , can be obtained by generalising the process, i.e. applying a second-order mixed derivative of  $M$  on a set of FORCs beginning at different  $H_r$  (Fig. 4) (Mayergoyz, 1985):

$$\rho_{FORC}(H, H_r) = -\frac{1}{2} \frac{\partial^2 M(H, H_r)}{\partial H \partial H_r} \quad (H > H_r) \quad (1)$$

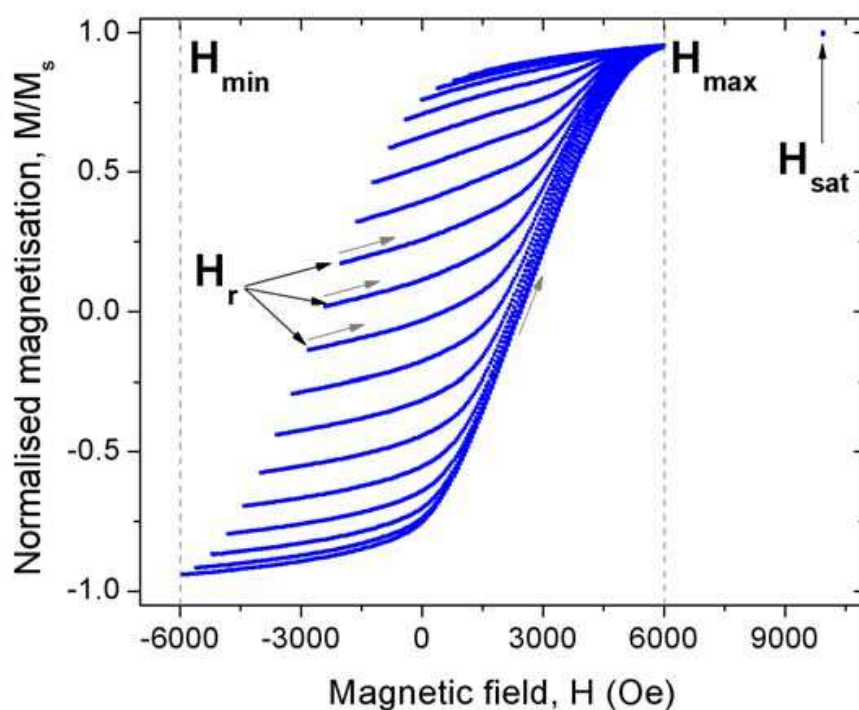


Fig. 4. Set of experimental first-order reversal curves. For practical reasons, only one curve out of four is shown. (CoFe nanowire array,  $d = 15$  nm,  $D = 55$  nm,  $L = 1.6$   $\mu$ m, axial direction,  $\Delta H = 50$  Oe,  $\Delta H_r = 100$  Oe)

In order to obtain the complete representation of the magnetisation reversal, the reversal field values cover the hysteretic area of the major hysteresis curve, from  $H_{min}$  to  $H_{max}$ . To accelerate the acquisition time, no measurement is taken between  $H_{max}$  and the saturation field. Also, experimentally, one should introduce a pause in the measurement at the saturation and reversal fields, long enough in order to avoid any magnetic viscosity effect. For metallic nanowires, 5 to 10 seconds proved to be sufficient (Béron, 2008). The choice of the experimental field steps  $\Delta H$  (between consecutive data on the FORC) and  $\Delta H_r$  (between different FORC) is the result of a trade-off between the FORC result precision and the measuring time. In order to optimise the experiment, these field steps can be varied according to the precision needed in different regions, but the  $\Delta H_r/\Delta H$  ratio should be kept between 1 (high hysteresis susceptibility) and 2.5 (low hysteresis susceptibility) (Béron et al., 2006).

Before calculating equation (1), the FORCs are extrapolated in a way which minimises the discontinuity at  $H = H_r$ , created by the lack of data taken in the  $H < H_r$  region (Béron et al., 2007). The FORC distribution then gives only and completely the information related to the irreversible processes (mathematical hysterons with  $H_c \neq 0$ ). The characterisation of the reversible processes can be done through the calculation of a reversibility indicator  $\eta$  (Fig. 5) (Béron et al., 2007):

$$\eta(H = H_r) = \frac{\chi_{FORC}(H = H_r)}{\chi_{Hyst}(H = H_r)} \quad (2)$$

A value of  $\eta = 0$  corresponds to a completely irreversible process and of  $\eta = 1$  to a fully reversible process.

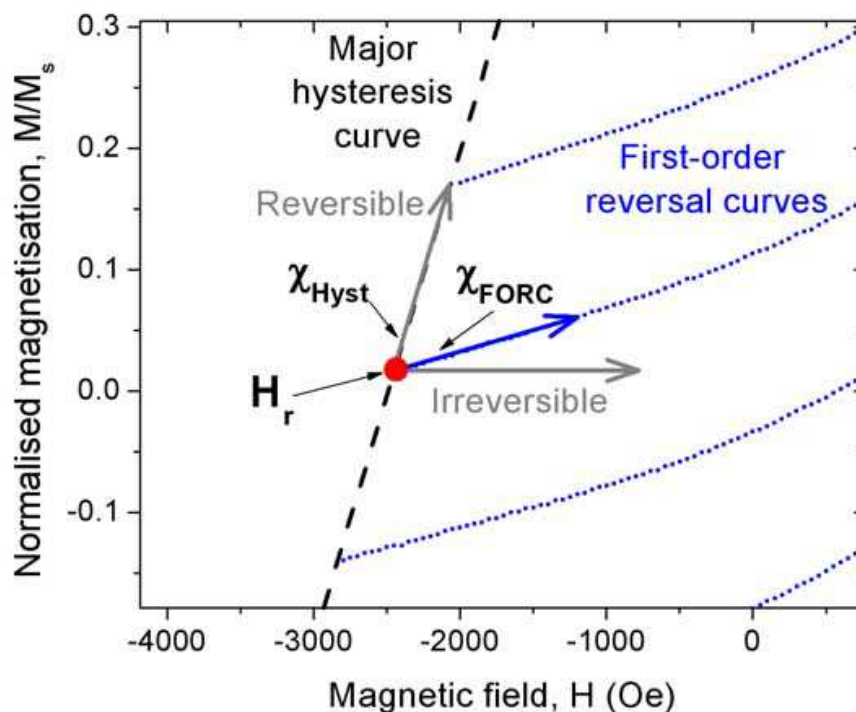


Fig. 5. Calculation of the reversibility indicator  $\eta$  at a given reversal field  $H_r$ . (Zoom of Fig. 4)

## 2.2 Analysis of results

Information about both reversible and irreversible processes can be combined in a graphical representation called “FORC result” (Fig. 6) (Béron, 2008). It consists of a contour plot of the FORC distribution  $\rho_{FORC}$ , with a scale going from blue (minimum  $\rho_{FORC}$ ) to red (maximum  $\rho_{FORC}$ ), which directly indicates the statistical distribution of the mathematical hysterons. In order to read the  $H_c$  and  $H_u$  mathematical hysteron parameters directly from the graph, it is convenient to execute a change of coordinates, to define a coercive field axis ( $H_c$ ) and an interaction field axis ( $H_u$ ) (see Fig. 3):

$$H_c = \frac{H - H_r}{2} \quad H_u = -\frac{H + H_r}{2} \quad (3)$$

In the classical Preisach model approach, the  $H_c$  and  $H_u$  cross-sections of the FORC distribution directly yield the coercivity and interaction field distributions. Even if this remains valid only for systems that respect the classical Preisach model requirements (which is not the case for most physical systems), the coordinate change remains appropriate; the FORC distribution generally spreads along the  $H_c$  and  $H_u$  axes. The reversibility indicator  $\eta$  is added to the FORC result as a greyscale strip, ranging from white (fully reversible behaviour) to black (fully irreversible behaviour). Two quantitative parameters can be defined on the FORC result: the  $H_c$  position of the FORC distribution maximum is called FORC coercivity ( $H_c^{FORC}$ ), while its half-width along the  $H_u$  axis is called global interaction field ( $\Delta H_u$ ) (Fig. 6) (Béron et al., 2008b). They will later be used for the FORC analysis along with the physical analysis model.

The FORC result analysis is generally the most difficult step in the use of the FORC method. The three major problems are 1) the FORC distribution represents the statistical distribution

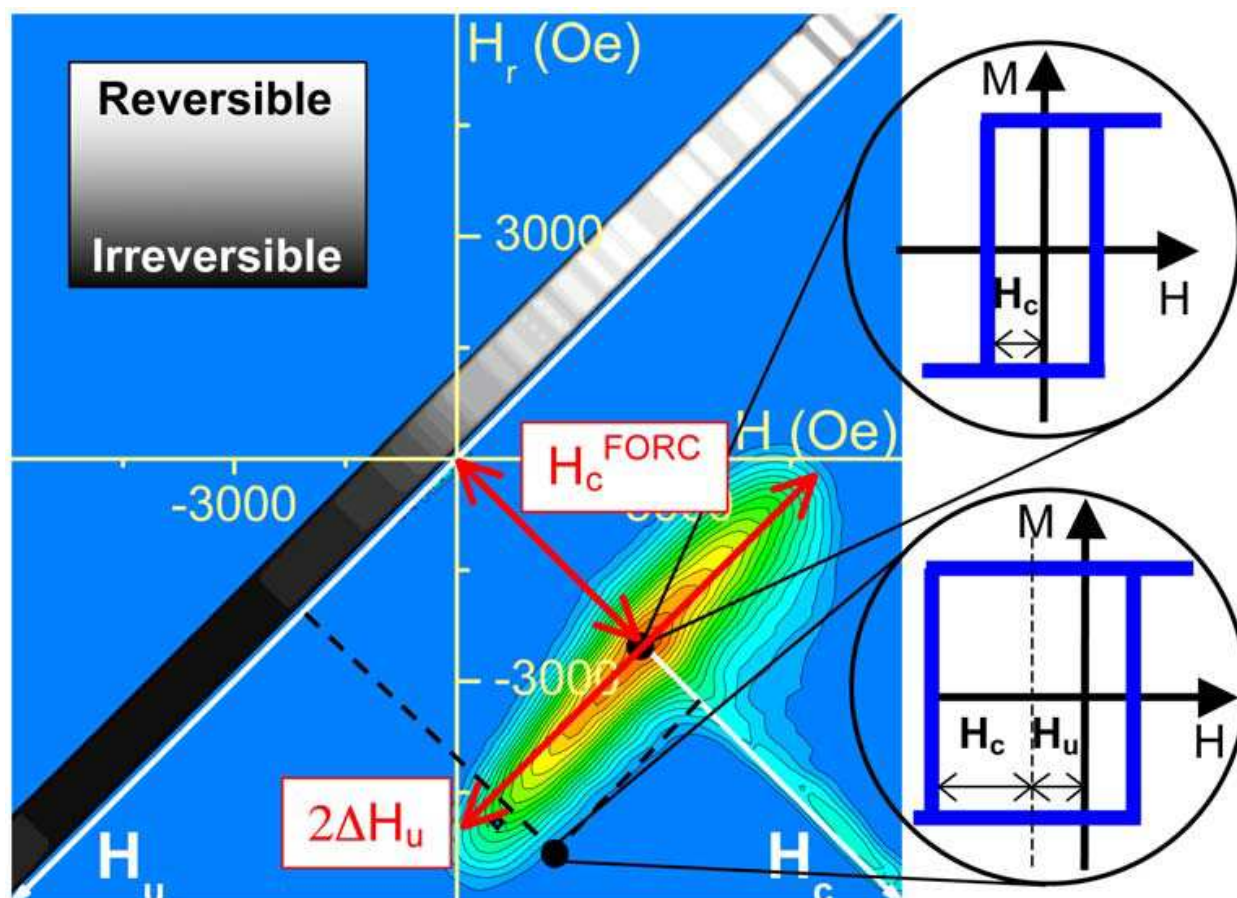


Fig. 6. FORC result (calculated from the set of FORCs shown in figure 4). Two mathematical hysteresis loops are represented, illustrating the use of the  $H_c$  and  $H_u$  axes to read the coercivity and bias field of the FORC distribution. The parameters  $H_c^{FORC}$  and  $\Delta H_u$  are also indicated.

of entities that do not necessarily have a physical meaning (the mathematical hysteresis loops), 2) the FORC distribution can be deformed by the presence of state-dependent interaction field during the reversal, such as a mean interaction field, and 3) different physical systems can exhibit identical FORC results. Several approaches to FORC interpretation, designed to overcome these problems, exist. One is called the physical analysis model (Béron et al., 2008a), which allows us to establish some quantitative relationships between the characteristics of a physical system and of the FORC result. It is achieved by using physically meaningful hysteresis loops, representing the supposed magnetic behaviour of the system entities, coupled with an interaction term, to simulate the global behaviour of the system. For example, the behaviour of each nanowire can theoretically be represented by the coherent rotation model (Stoner & Wohlfarth, 1948). The nanowire is approximated as an infinite cylinder where all the spins remain parallel to each other during the magnetisation reversal. This defines two different hysteresis loops, depending upon the applied field direction, that can be used in the physical analysis model (Fig. 7).

The FORC behaviour strongly depends upon the type of hysteresis loops. For example, for easy axis hysteresis loops, a coercivity distribution will spread the FORC distribution along the  $H_c$  axis (Fig. 8a). With an interaction field (and no coercivity distribution), the result depends upon its direction relative to the saturation magnetisation. An antiparallel interaction field (opposite to the magnetisation) will elongate the FORC distribution along the  $H_u$  axis (Fig. 8b), while a

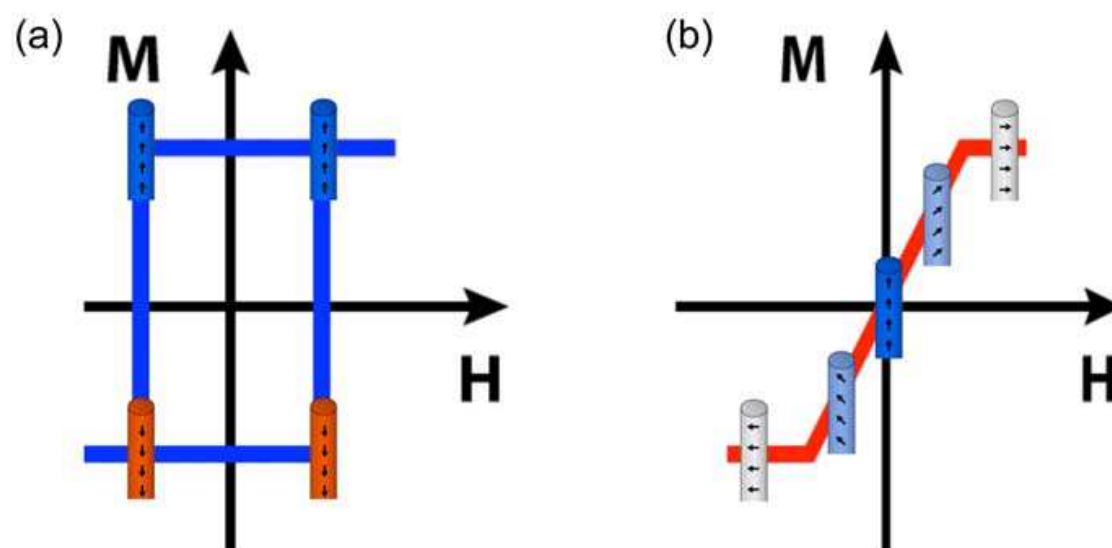


Fig. 7. Hysteron based on the theoretical behaviour of an individual nanowire, depending upon the applied field direction. (a) Axial applied field: easy axis hysteron (b) Transverse applied field: hard axis hysteron

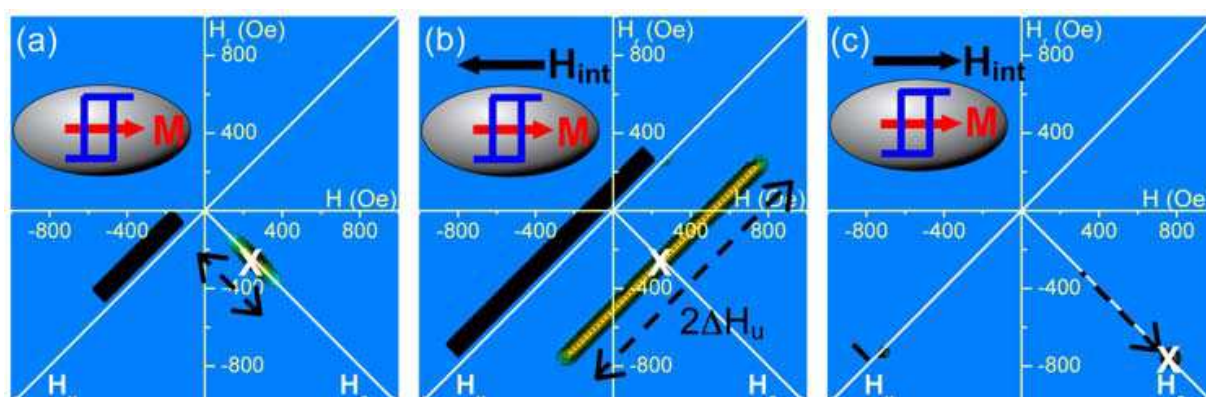


Fig. 8. Simulated FORC results with easy axis hysterons. The  $H_c^{FORC}$  parameter is indicated as a white X. (a) Normal coercivity distribution, no interaction field (b) Antiparallel mean interaction field, no coercivity distribution (c) Parallel mean interaction field, no coercivity distribution

parallel interaction field will have as consequence to translate it toward higher values on the  $H_c$  axis (Fig. 8c) (Béron et al., 2008a). These simulations showed that the shape of the FORC distribution, if clear and intuitive for a simple system (only one characteristic, i.e. fully reversible or irreversible, coercivity distribution or mean interaction field), quickly becomes more complex and far from the direct interpretation based on the mathematical hysterons.

From a quantitative point of view, the average individual coercivity of easy hysterons can be extracted from the FORC result by taking the  $H_c$  coordinate at  $H_u = 0$  of the maximum of the FORC distribution, i.e. the  $H_c^{FORC}$  parameter, at  $H_u = 0$ . This remains valid for systems with coercivity distribution (no interaction field, Fig. 8a) or with antiparallel interaction field (no coercivity distribution, Fig. 8b). In the limit of total absence of both coercivity and interaction field distributions, the half-width of the FORC distribution elongation ( $\Delta H_u$ ) is equal to the absolute value of the coefficient parameter  $k$  ( $k < 0$ ) of a mean interaction field, which yields the value of interaction field at saturation ( $M = M_s$ ) (Fig. 8b):

$$H_{\text{int}} = k \frac{M}{M_s} \quad (4)$$

Finally, in the presence of a mean parallel interaction field ( $k > 0$ ) and no coercivity distribution, the  $H_c^{\text{FORC}}$  value is the sum of the individual coercivity and the coefficient  $k$ . (Fig. 8c) (Béron et al., 2008a).

### 3. Fabrication of nanowire arrays

Nanowire arrays may be fabricated by electrodeposition of metallic ions into the cylindrical pores of a dielectric template (Masuda & Fukuda, 1995). This deposition technique is economic, fast, versatile and does not require high vacuum facilities. A three electrodes configuration is typically used, the sample being used as the working electrode while the counter electrode is in platinum (Pt) (Fig. 9). The applied potential is given with respect to that of the reference electrode, usually a saturated calomel, because of the stability of its potential.

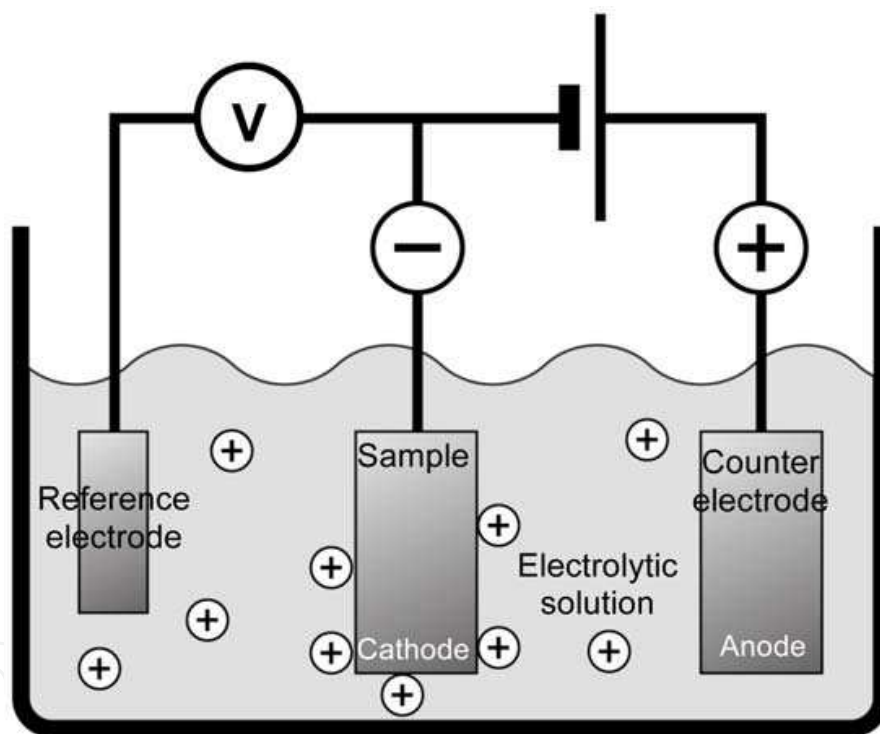


Fig. 9. Schematic of an electrolytic cell used in the electrodeposition of the ferromagnetic nanowires.

The nanoporous dielectric template is typically made of anodised aluminium (alumina) (O'Sullivan & Wood, 1970), ion bombarded polycarbonate (Ferain & Legras, 2003) or diblock copolymer (Thurn-Albrecht et al., 2000). It is important that the pores be of constant diameter, parallel to each other, and perpendicular to the template surface. The most widely used template is currently alumina, mainly due to the ease of tailoring the template geometry (pore diameter, length and interpore distance) in laboratory, to the hexagonal arrangement of the pores, and to the rigidity of the template. They are fabricated in a two-step anodisation process (Fig. 10) (Masuda & Fukuda, 1995; Pirota et al., 2004; Zhao et al.,

2007). A cleaned aluminium substrate is first slowly anodised in an acidic bath under constant voltage. Since the pore order is getting more regular during this process, the initial layer of alumina (aluminium oxide) is chemically etched, before a second anodisation is performed, under the same conditions as the first. Finally, a chemical etch can enlarge the pores, if needed.

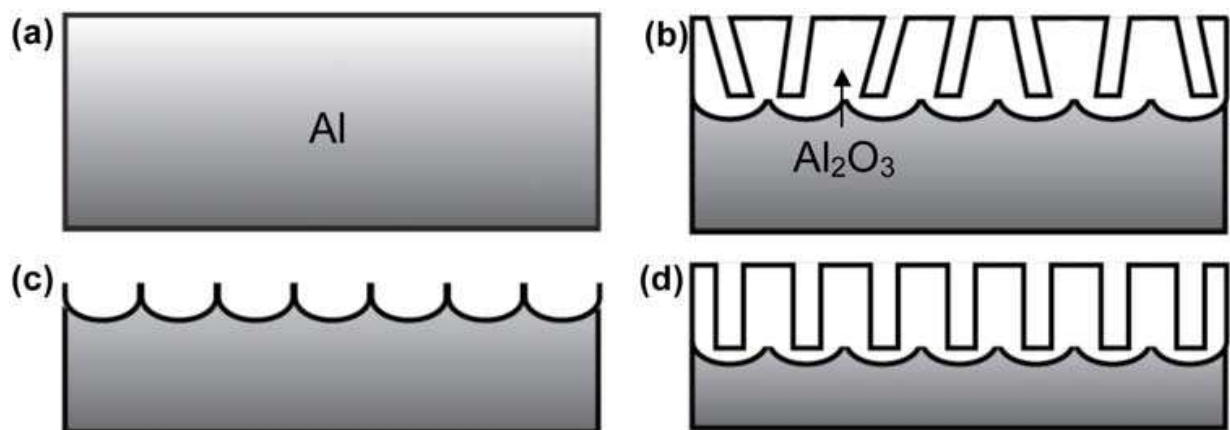


Fig. 10. Schematic of the two-step anodisation process for fabricating nanoporous anodised aluminium templates. (a) Electropolished Al substrate (b) First anodisation (c) Etching of the alumina layer (d) Second anodisation

The samples discussed here were all fabricated in commercially available alumina templates (thickness = 60  $\mu\text{m}$ , pore diameter = 175 nm, interpore distance = 300 nm, pore density =  $10^9$  pores/cm<sup>2</sup>, figure 11a). However, due to the filtration purpose of these templates, the pores split into multiple smaller pores in the first 500 to 700 nm (Fig. 11b). This region was therefore removed by mechanical polishing before magnetic characterisation, in order to make the magnetic behaviour more uniform.

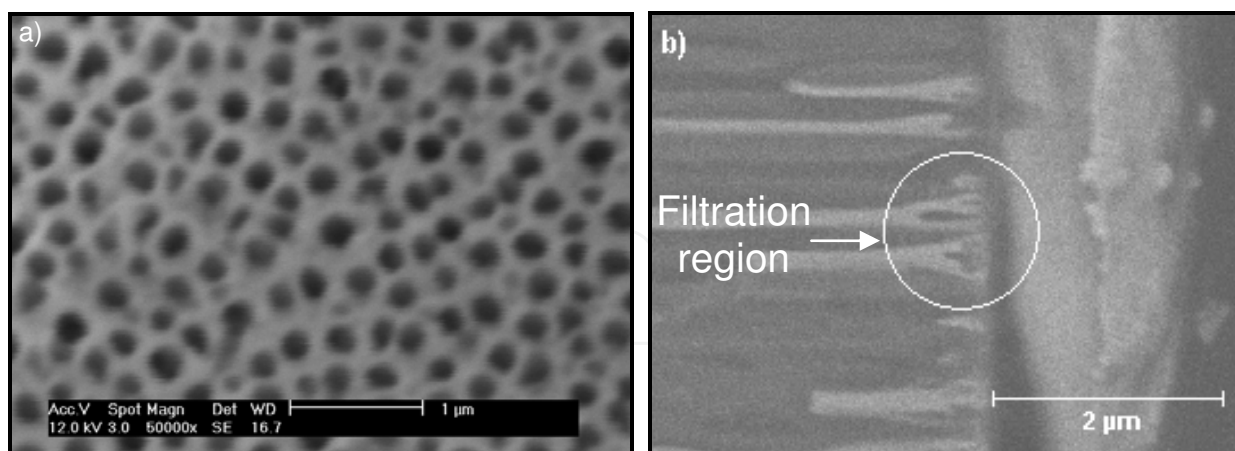


Fig. 11. Commercial alumina template (Anodisc™ 0.02  $\mu\text{m}$ ) (a) Top view (b) Cross-sectional view of the pore bottom, showing the filtration region, removed before magnetic characterisation.

The pulse-current electrodeposition technique was used for the fabrication of the uniform nanowires. This technique consists of sending short current pulses (8 ms), during which the deposition occurs, followed by a pause (152 ms) (Ciureanu et al., 2005) (Fig. 12a). It avoids the formation of composition gradients along the nanowires (Nielsh et al., 2000), prevents

formation of hydrogen in the pores and therefore allows uniform filling of the pores. Neither composition (Ni and CoFeB) exhibited large magnetocrystalline anisotropy, since the CoFeB was amorphous and the magnetocrystalline anisotropy of Ni is low. Multilayer nanowires can also be fabricated in an electrolytic bath containing all the elements to be deposited (Blondel et al., 1994; Piraux et al., 1994). In this case, the potential is alternated between two values, where the deposition of each material is favoured for one value of potential (Alper et al., 1993) (Fig. 12b). The non-magnetic metal is kept dilute in the solution to avoid excessive inclusion in the magnetic layer. Ni/Cu nanowires were fabricated by this method (-1 V for Ni, -0.56 V for Cu), varying the Cu/Ni ratio from 0.3 to 1.17 (Carignan et al., 2007).

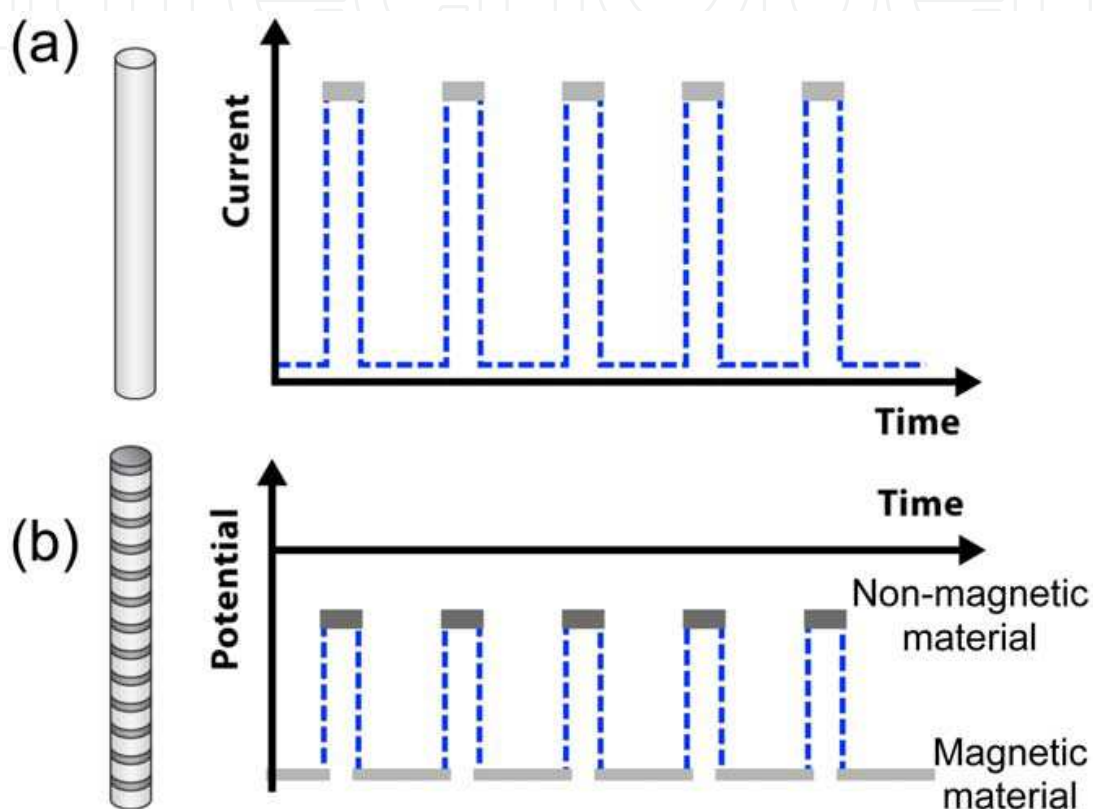


Fig. 12. Programmed electrical parameters for the electrodeposition process. (a) Pulse-current electrodeposition (b) Alternating potential. The grey lines represent the deposition of the different materials.

#### 4. Experimental FORC results

The experimental FORC results for four different nanowire arrays, two uniform (Ni and CoFeB) and two multilayer, are presented in Figs 13-16 as typical examples. Despite the fact that the nanowire arrays have the same geometry, one may easily see that they exhibit different magnetic behaviour. They were therefore chosen in order to exhibit the versatility of the FORC method. They are all characterised by the presence of both reversible and irreversible processes, which complicates their quantitative analysis.

In an axial applied field, the FORC distribution of elongated cylinders always exhibits the same kind of shape, i.e. narrow in the  $H_c$  direction and highly elongated along the  $H_u$  axis. According to the coherent rotation model, each nanowire could theoretically be represented by an easy axis hysteron, due to the large shape anisotropy. Therefore, the interpretation of

the FORC distribution shape, according to the coherent rotation model, would lead to the conclusion that all the nanowires have almost the same coercivity, with the geometric non-uniformity leading to a narrow coercivity distribution. They are subject to a high antiparallel interaction field, created by the dipolar interactions, as seen from the elongated distribution along the  $H_u$  axis. However, it will be seen in section 5 that the coherent rotation model fails to account for the low coercivity of the arrays and for several features of the FORC results. The FORC distribution shape obtained under a transverse applied field varies significantly, suggesting radically different magnetic behaviour depending upon the nanowire array properties.

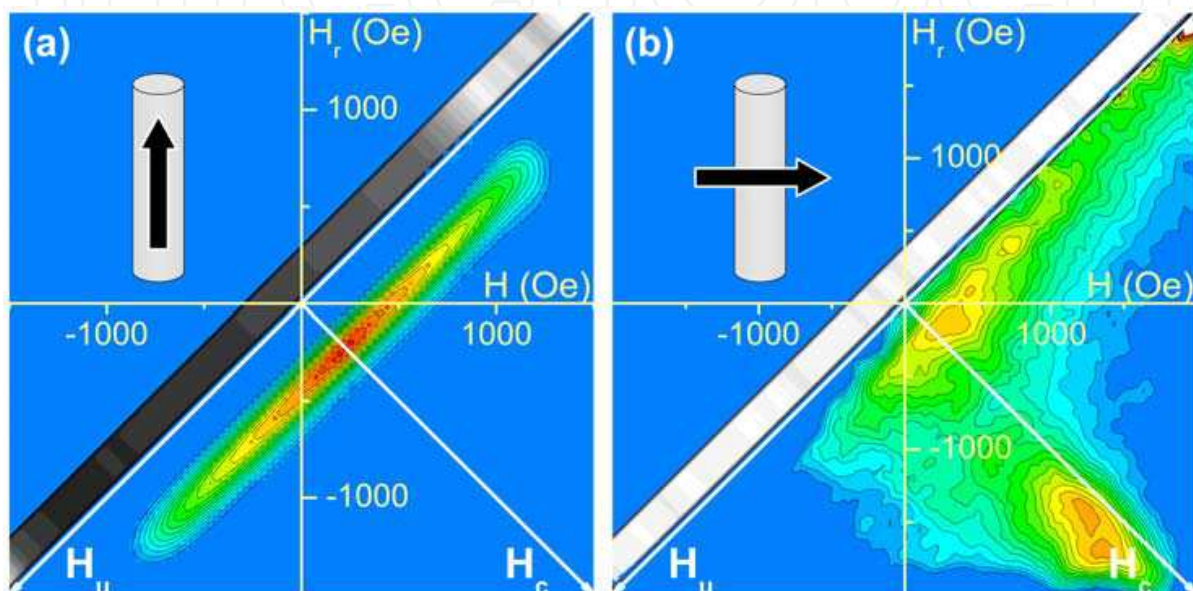


Fig. 13. FORC results for a Ni nanowire array ( $L = 19 \mu\text{m}$ , axial easy axis). Applied field (a) axial and (b) transverse.

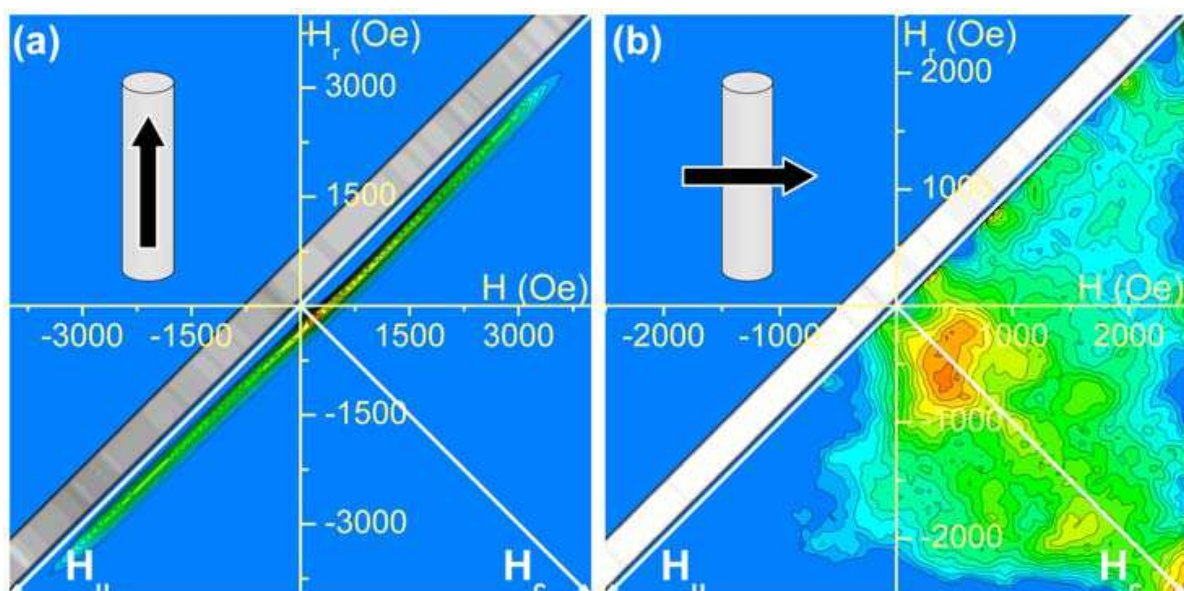


Fig. 14. FORC results for a CoFeB nanowire array ( $L = 25 \mu\text{m}$ , axial easy axis). Applied field (a) axial and (b) transverse.

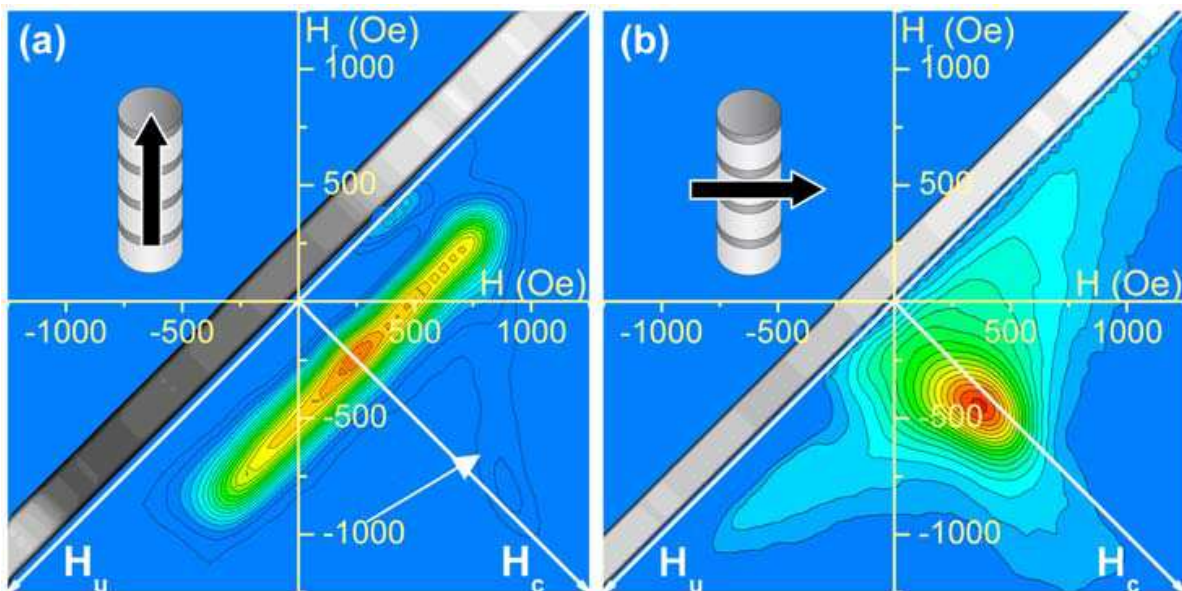


Fig. 15. FORC results for a Ni/Cu nanowire array ( $L = 32.5 \mu\text{m}$ , Ni nanodisc thickness = 50 nm, Cu nanodisc thickness = 15 nm, Cu/Ni thickness ratio = 0.3, axial easy axis). Applied field (a) axial and (b) transverse.

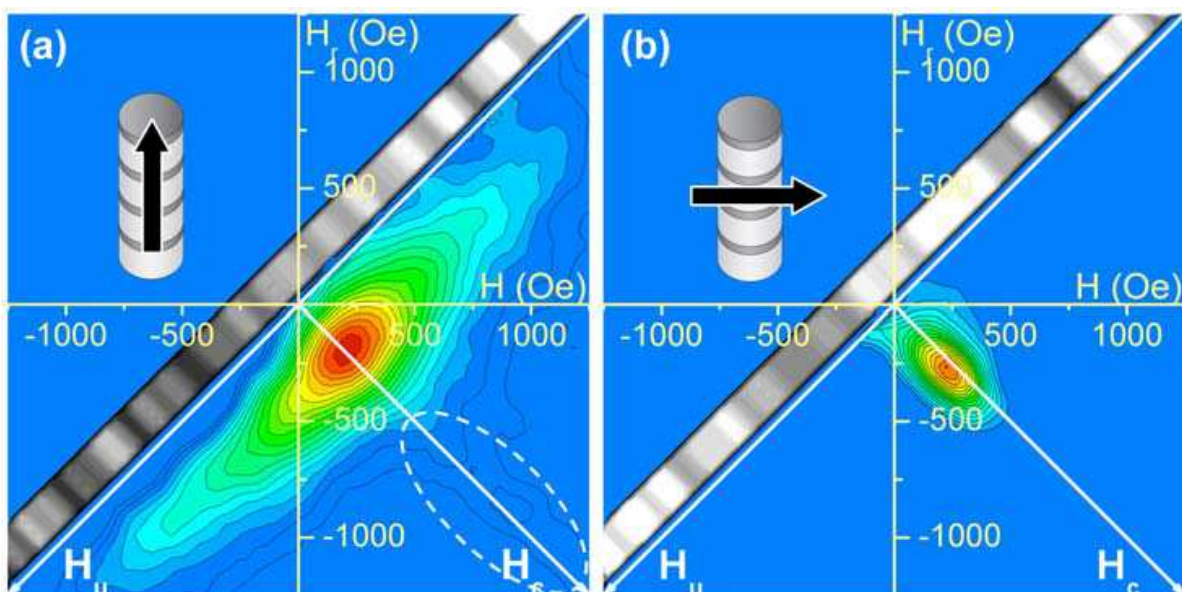


Fig. 16. FORC results for a Ni/Cu nanowire array ( $L = 3.25 \mu\text{m}$ , Ni nanodisc thickness = 30 nm, Cu nanodisc thickness = 35 nm, Cu/Ni thickness ratio = 1.17, transverse easy axis). Applied field (a) axial and (b) transverse.

## 5. Extracting individual nanowire properties

### 5.1 Individual nanowire coercivity/interaction field

In strongly interacting systems, like ferromagnetic nanowire arrays, the extraction of the interaction field and of individual coercivities have to be done together. This is because the interaction field modifies the FORC distribution, which can then no longer be analysed using the classical Preisach model, in which the coercive and interaction fields are

independent. In the specific case of nanowire arrays, both FORC results obtained with axial and with transverse applied fields should be considered simultaneously.

#### *Axial applied field*

When the axial FORC distribution is qualitatively equivalent to that presented in Fig. 8b, as is the case for all the experimental distributions presented above (Figs 13-16), it suggests a narrow coercivity distribution and a net antiparallel interaction field. This allows us to use  $H_c^{FORC}$  as a first approximation to the average coercivity of the individual nanowires. However, two cases may occur for which this approximation is no longer adequate: 1) if the coercivity distribution is large enough to disturb the FORC distribution, inducing a second branch (Fig. 15a, shown by the arrow) or enlarging it along the  $H_c$  axis (Fig. 16a); 2) if both the reversibility indicator and the antiparallel interaction field are large (Fig. 14a); their simultaneous presence in a system will shift the entire FORC distribution towards higher coercivity, in proportion to these two values (Béron, 2008). In the later case, the  $H_c^{FORC}$  approximation should be corrected before being used as the average individual nanowire/nanodisc coercivity.

When  $H_c^{FORC}$  satisfies the conditions for it to represent the individual wire coercivity, the net value of the axial interaction field at saturation is then well described by  $\Delta H_u$ , defined as the half-width at half-height of the uniform part of the  $\Delta H_u$  cross-section (Fig. 17). Good agreement (Béron et al., 2008b) was found between the experimental  $\Delta H_u$  values of uniform nanowires (Figs 13-14a) and the predicted values of interaction field at saturation from a micromagnetic model (Clime et al., 2006) and from an effective field model (Carignan et al., 2007).

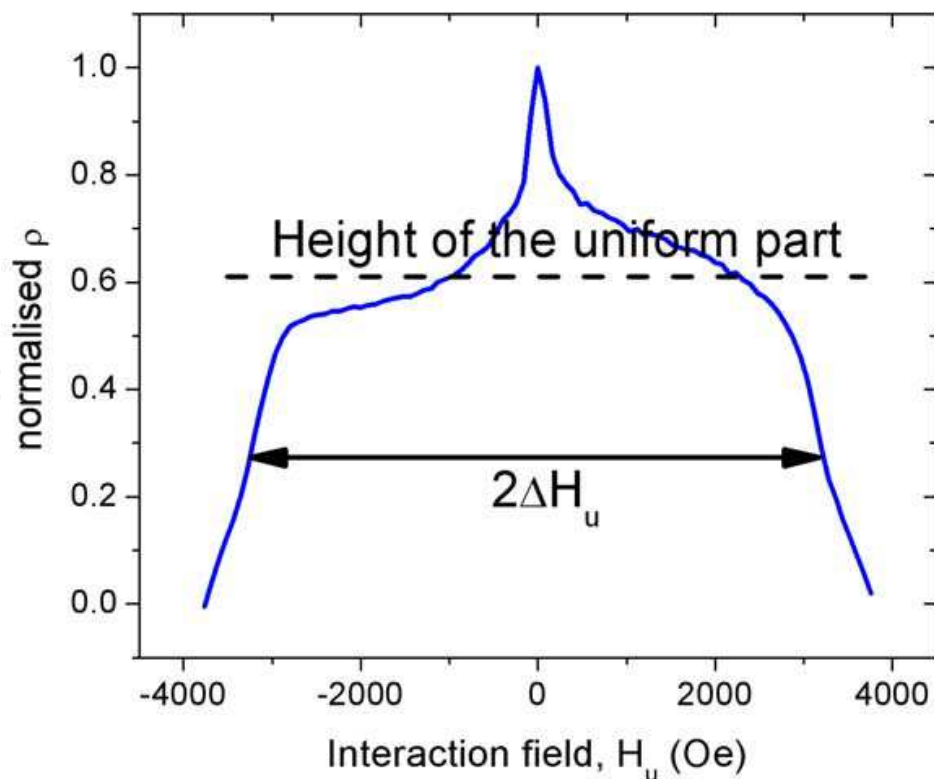


Fig. 17. Axial FORC distribution cross-section along the  $H_u$  axis and its respective  $\Delta H_u$  value. (CoFeB nanowire array, see Fig. 14a)

If we assume a uniform, antiparallel interaction field, described by Eq. (4), we expect a FORC distribution that is straight and parallel to the  $H_u$  axis and with a flat  $H_u$  cross-section (Fig. 18a). Spatial non-uniformity in the interaction field induces some deviations in this distribution. Three kinds of deviation can be easily identified.

First, a spatial distribution of interaction field caused by the array border can induce a central peak in the  $H_u$  cross-section (Fig. 18b). Most of the nanowires are submitted to a dipolar field that can be treated as a mean interaction field. However, the array is not infinite. The nanowires located at the array borders, where the lack of neighbours induces a smaller interaction field, can complete their reversal when this field is still relatively weak. This results in a peak at the centre of the cross-sections along  $H_u$  (present for all the experimental results). This hypothesis was confirmed by noting that the amplitude of the central peak is significantly reduced when very large samples are measured. Therefore, characterisation should always be carried out using the largest area possible, in order to avoid this effect.

Second, if the antiparallel interaction field decrease allows the preponderance of a parallel interaction field (for example, the dipolar field between nanodiscs within a multilayer nanowire), then, in addition to the central peak, another distribution can appear, reflecting this parallel interaction field effect (ex.: distribution of higher coercivity, circled on figure 16a).

Finally, for arrays of radius significantly larger than the nanowire length and for which the condition  $L/2D \gg 1$  is satisfied, then the interaction field decreases near the nanowire extremities (Carignan et al., 2007). Therefore, depending upon the applied field direction (positive or negative), the magnetisation reversal is favoured either by a maximal or minimal value of interaction field, inducing a non-linearity in the FORC distribution (Fig. 18c). This non-linearity is experimentally more visible in the case of CoFeB nanowires (Fig. 14a) than for Ni (Fig. 13a), because higher saturation magnetisation leads to larger interaction fields.

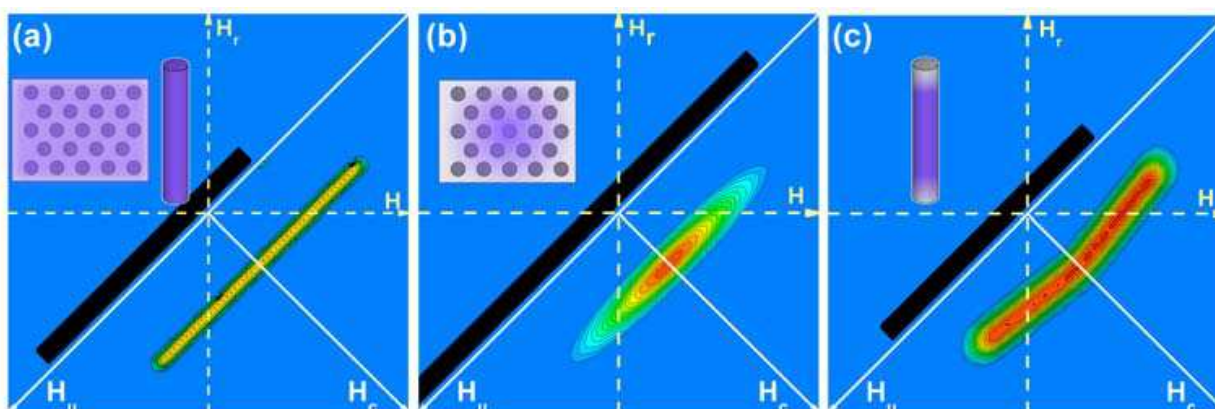


Fig. 18. Simulated FORC results for several configurations of spatial distribution of interaction field. (a) Uniform mean interaction field (b) Distribution in the array (c) Distribution along the nanowires

#### *Transverse applied field*

With a transverse applied field on an infinite array, the interaction field at saturation is theoretically parallel to  $M$ , and equal to the half of the axial interaction field (Carignan et al., 2007). This value has been successfully used to fit the transverse major hysteresis curves of uniform nanowires (Béron, 2008). For FORC distributions that are narrow on the  $H_c$  axis, as

in figures 15b and 16b, the transverse individual coercivity is indirectly accessible through use of the analysis illustrated in Fig. 8c. Subtracting the half value of the axial  $\Delta H_u$  from the transverse  $H_c^{FORC}$  value allows us to retrieve the coercivity of individual nanodiscs in multilayer nanowires (Béron et al., 2008c).

## 5.2 Effective nanowire array anisotropy

In cases where the sum of the minimum values of the reversibility indicator  $\eta$  (Béron et al., 2007, see fig. 19a) in axial and transverse applied field is around 1, an indication of the

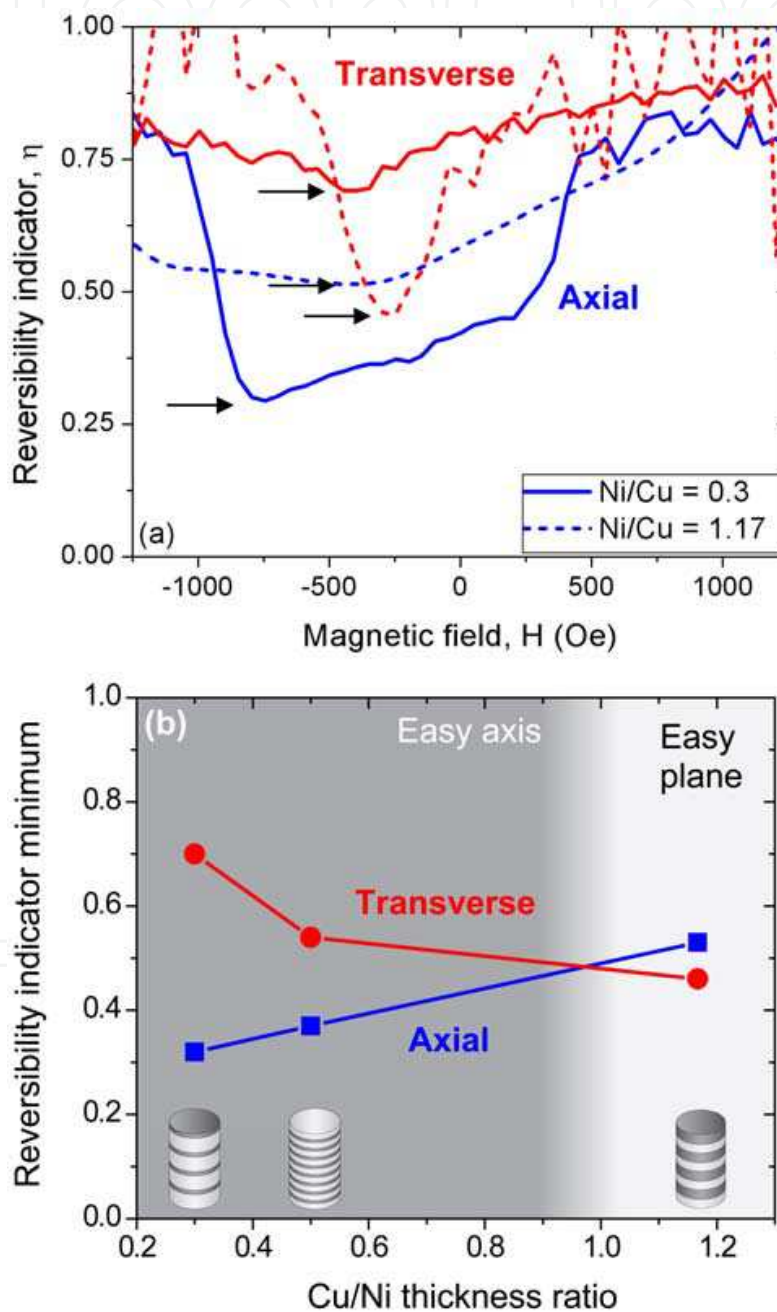


Fig. 19. (a) Reversibility indicator as a function of the reversal field for multilayer nanowires. The position of the minimum is indicated. (b) Reversibility indicator minimum as a function of the Cu/Ni thickness ratio. The cross-over indicates the change of easy axis direction.

overall anisotropy of the nanowire array can be obtained by the FORC method. Otherwise, other processes contribute to the reversibility indicator and therefore the minimum value of  $\eta$  cannot be used to adequately characterise the effective nanowire array anisotropy. When the sum is around 1, the reversibility being lower along an easy direction, the lowest  $\eta$  minimum value indicates an easy direction. A cross-over between the  $\eta$  minimum value curves, occurring when the array is magnetically isotropic, implies a change in the easy axis direction (Fig. 19b) (Béron et al., 2008c). This result for multilayer nanowires is in agreement with those found from the major hysteresis curves and ferromagnetic resonance measurements, as well as demagnetisation factor modelling (Carignan et al., 2007).

### 5.3 Magnetisation reversal process

Quantitative knowledge of the interaction field, average individual coercivity and overall array anisotropy, along with the FORC distribution shape, can help us determining the magnetisation reversal process. However, one has to remember that the FORC method does not directly give the type of magnetisation reversal occurring in the sample and so has to be used as a tool which suggests a probable mechanism, since systems reversing by different means can exhibit the same FORC result.

#### *Axial applied field*

For uniform nanowire arrays and axial applied field, coherent rotation reversal of individual nanowires leads to purely irreversible behaviour, with a unique value of  $H_c^{FORC}$  equal to the shape anisotropy field (as in Fig 8b). Another possible reversal mechanism is by nucleation-propagation of a domain wall, which has been observed for the reversal of individual nanowires (Wernsdorfer et al., 1996; Hertel, 2001) (Fig. 20a). Then, the FORC result can exhibit some reversibility, a coercivity lower than the shape anisotropy field and a second distribution of coercivity near saturation, associated with annihilation of the domain walls (Béron, 2008) (circled on Fig. 20b). The FORC results presented in Figs 13a and 14a exhibit these three characteristics and, therefore, nucleation-propagation magnetisation reversal mechanism is more likely in these cases than coherent rotation.

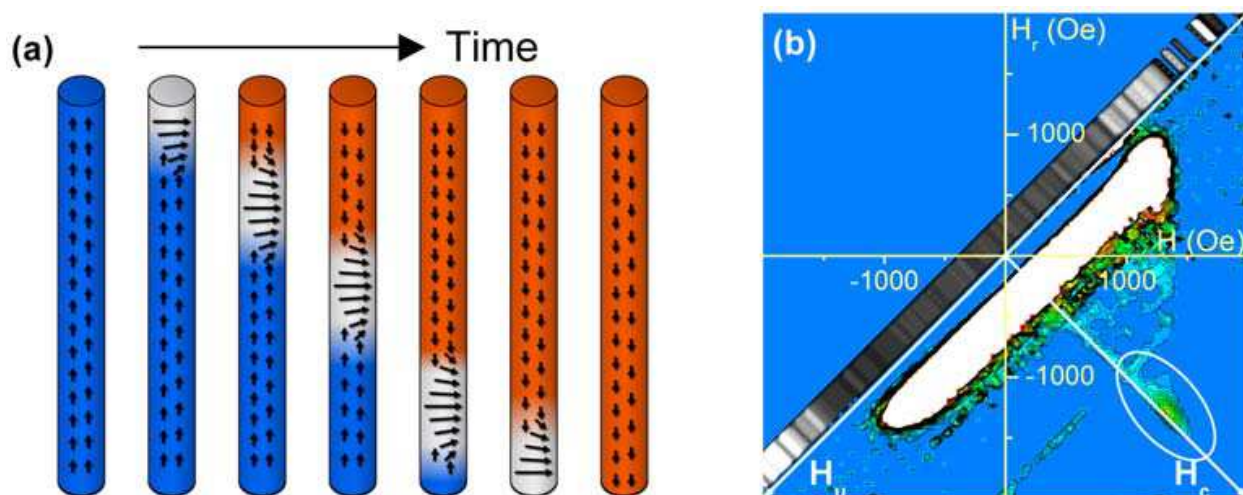


Fig. 20. (a) Schematic of the nucleation-propagation of a domain wall. (b) Ni axial FORC result, where the scale has been adjusted in order to show the second distribution of lower intensity (circled), generated by nucleation-propagation reversal.

### *Transverse applied field*

For an applied field transverse to the nanowire axis, the coherent rotation model predicts fully reversible behaviour for a uniform individual nanowire, being along a hard direction, and no other FORC distribution. The existence of irreversible processes in Figs 13b and 14b, even in low proportion (1 - 4%), indicates that at least one other mechanism is present. This process could be the irreversible reversal of the domain walls created between regions decoupled enough to allow the magnetisation to rotate coherently freely toward one or the other nanowire extremity (Fig. 21) (Henry et al., 2002; Hertel, 2001). Other phenomena, such as closure domains at nanowire extremities, could also contribute to the non-null FORC distribution.

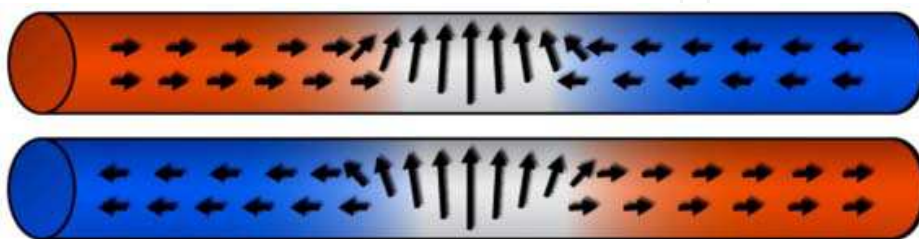


Fig. 21. Schematic of 180° domain walls created during transverse magnetisation reversal. The irreversible reversal could account for the irreversible FORC distribution in Figs. 13b and 14b.

Other types of FORC results are possible and have to be analysed individually, based on the available information concerning the transverse magnetic behaviour of the array. For example, for multilayer nanowires, the FORC result presented in Fig. 15b was attributed to a mixture of coherent and incoherent rotation, the favourable conditions for one or the other changing during the reversal, while Fig. 16b was interpreted as an abrupt, irreversible reversal, caused by field applied along an easy direction (Béron et al., 2008c).

## 6. Conclusion

The unique structure of ferromagnetic nanowire arrays gives them interesting properties for various applications, ranging from high-density memory to high frequency devices. They may be fabricated by electrodeposition, a process which is fast, cheap and versatile. From a magnetic point of view, their behaviour is mainly governed by a competition between the shape anisotropy (an individual property of each nanowire) and the dipolar interaction field (an effect of the network). Therefore, it is important to be able to characterise both the individual and global properties of nanowire arrays, in order to understand their magnetic behaviour and to implement them adequately in devices.

This experimental characterisation can be achieved in one single step on the whole array, by using the very promising first-order reversal curve (FORC) method. The acquisition of several minor hysteresis curves allows us to record and discriminate the magnetisation reversal of each nanowire, ultimately yielding a representation of the reversal of all the nanowires. From this representation (the FORC result) and the help of the physical analysis model (based on predicted behaviour), one can extract valuable information, usually difficult to obtain experimentally. The half-width of the FORC distribution elongation ( $\Delta H_u$ ) along the interaction field axis ( $H_u$ ) gives the value of the interaction field at saturation, while a spatial distribution of this field modifies its shape. The spatial non-homogeneity can

be in the array (border effect), which induces a central peak in the FORC distribution, or along the nanowires (extremity effect), which breaks the FORC distribution linearity along the  $H_u$  axis. An approximation of the average individual coercivity of the nanowires can be obtained by taking the position of the maximum of the FORC distribution on the coercivity axis ( $H_c$ ) ( $H_c^{FORC}$ ). This approximation remains valid if the coercivity distribution is narrow, and both the reversibility indicator and the antiparallel interaction field are not too large. Also, in the presence of a parallel interaction field, its saturation value has to be subtracted from  $H_c^{FORC}$  in order to reflect the individual coercivity. Finally, a quantitative evaluation of the effective anisotropy of the array is accessible through the minimum value of the reversibility indicator function of the reversal field, if the sum from axial and transverse applied fields is close to 1.

The versatility of the FORC method has been demonstrated here by discussing experimental results for nanowire arrays with different compositions (Ni and CoFeB), and thus different saturation magnetisation, and different structures (uniform and multilayer), all under both axial and transverse external applied fields. However, the application range of the FORC method is not confined to the two principal directions (axial and transverse) of the array. The physical analysis model can also be employed for the study of the magnetic behaviour as a function of the applied field angle (Béron et al., 2009a). The tridimensional and highly reversible magnetisation reversal process in this case led to the development of a novel variant of the FORC method, vector FORC, where both magnetisation components, parallel and perpendicular to the applied field direction, are used. This allows us to adequately follow and characterise reversible magnetisation rotation in three dimensions (Béron et al., 2009b).

## 7. References

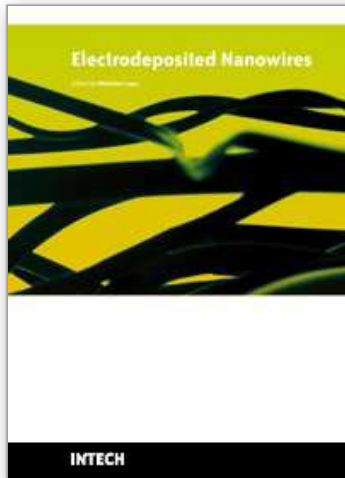
- Almawlawi D.; Coombs N. & Moskovits M. (1991). Magnetic properties of Fe deposited into anodic aluminum oxide pores as a function of particle size. *Journal of Applied Physics*, Vol. 70, No. 8, October 1991, 4421-4425, 0021-8979
- Alper, M.; Attenborough, K.; Hart, R.; Lane, S.J.; Lashmore, D.S.; Younes, C. & Schwarzacher, W. (1993). Giant magnetoresistance in electrodeposited superlattices. *Applied Physics Letters*, Vol. 63, No. 15, October 1993, 2144-2146, 0003-6951
- Béron, F.; Clime, L.; Ciureanu, M.; Ménard, D.; Cochrane, R.W. & Yelon A. (2006). First-order reversal curves diagrams of ferromagnetic soft nanowire arrays. *IEEE Transactions on Magnetics*, Vol. 42, No. 10, October 2006, 3060-3062, 0018-9464
- Béron, F.; Clime, L.; Ciureanu, M.; Ménard, D.; Cochrane, R.W. & Yelon A. (2007). Reversible and quasireversible information in first-order reversal curve diagrams. *Journal of Applied Physics*, Vol. 101, No. 9, May 2007, 09J107, 0021-8979
- a - Béron, F.; Ménard, D. & Yelon, A. (2008). First-order reversal curve diagrams of magnetic entities with mean interaction field: A physical analysis perspective. *Journal of Applied Physics*, Vol. 103, No. 7, April 2008, 07D908, 0021-8979
- b - Béron, F.; Clime, L.; Ciureanu, M.; Ménard, D.; Cochrane, R.W. & Yelon A. (2008). Magnetostatic interactions and coercivities of ferromagnetic soft nanowires in uniform length arrays. *Journal of Nanoscience and Nanotechnology*, Vol. 8, No. 6, June 2008, 2944-2954, 1533-4880

- c - Béron, F.; Carignan, L.-P.; Ménard, D. & Yelon, A. (2008). Magnetic Behavior of Ni/Cu Multilayer Nanowire Arrays Studied by First-Order Reversal Curve Diagrams. *IEEE Transactions on Magnetics*, Vol. 44, No. 11, November 2008, 2745-2748, 0018-9464
- Béron, F. (2008). *Propriétés magnétostatiques de réseaux de nanofils via les courbes de renversement du premier ordre*, Ph. D. thesis, Université de Montréal, Montréal, Canada
- a - Béron, F.; Carignan, L.-P.; Pirola, K.R.; Knobel, M.; Ménard, D. & Yelon, A. (2009). Magnetization reversal of ferromagnetic nanowire arrays studied by angular FORC measurements, 2009 IEEE International Magnetics Conference (INTERMAG), Sacramento, USA, May 2009
- b - Béron, F.; Pirola, K.R.; Knobel, M.; Ménard, D. & Yelon, A. (2009). Vector first-order reversal curve (FORC) results, International Conference on Magnetism 2009 (ICM), Karlsruhe, Germany, July 2009
- Blondel, A.; Meier, J.P.; Doudin, B. & Ansermet, J.-P. (1994). Giant Magnetoresistance of Nanowires of Multilayers, *Applied Physics Letters*, Vol. 65, No. 23, December 1994, 3019-3021, 0003-6951
- Carignan, L.-P.; Lacroix, C.; Ouimet, A.; Ciureanu, M.; Yelon, A. & Ménard, D. (2007) Magnetic anisotropy in arrays of Ni, CoFeB, and Ni/Cu nanowires. *Journal of Applied Physics*, Vol. 102, No. 2, July 2007, 023905, 0021-8979
- Ciureanu, M.; Béron, F.; Clime, L.; Ciureanu, P.; Yelon, A.; Ovari, T.A.; Cochrane, R.W.; Normandin, F. & Veres, T. (2005). Magnetic properties of electrodeposited CoFeB thin films and nanowire arrays, *Electrochimica Acta*, Vol. 50, No. 2, August 2005, 4487-4497, 0013-4686
- Clime, L.; Béron, F.; Ciureanu, P.; Ciureanu, M.; Cochrane, R.W. & Yelon A. (2006). Characterization of individual ferromagnetic nanowires by in-plane magnetic measurements of arrays. *Journal of Magnetism and Magnetic Materials*, Vol. 299, No. 2, April 2006, 487-491, 0304-8853
- Della Torre, E. (1966). Effect of Interaction on the Magnetization of Single Domain Particles, *IEEE Transactions on Audio and Electroacoustics*, Vol. AU-14, No. 2, June 1966, 86-92, 0018-9278
- Ferain, E. & Legras, R. (2003). Track-etch templates designed for micro- and nanofabrication. *Nuclear Instruments & Methods in Physics Research*, Vol. 208, August 2003, 115-122, 0168-583X
- Henry, Y.; Iovan, A.; George, J.-M. & Piroux, L. (2002). Statistical analysis of the magnetization processes in arrays of electrodeposited ferromagnetic nanowires, *Physical Review B*, Vol. 66, No. 18, November 2002, 184430, 1098-0121
- Hertel, R. (2001). Micromagnetic simulations of magnetostatically coupled nickel nanowires, *Journal of Applied Physics*, Vol. 90, No. 11, December 2001, 5752-5758, 0021-8979
- Hertel, R. & Kirschner, J. (2004). Magnetization reversal dynamics in nickel nanowires, *Physica B*, Vol. 343, No. 1-4, January 2004, 206-210, 0921-4526
- Lavín, R.; Denardin, J.C.; Escrig, J.; Altbir, D.; Cortés, A. & Gómez, H. (2008). Magnetic characterization of nanowire arrays using first order reversal curves, *IEEE Transactions on Magnetics*, Vol. 44, No. 11, November 2008, 2808-2811, 0018-9464

- Le Bon, G. (1895). *Psychologie des foules*, Les Presses universitaires de France, 978-2130542971 Paris, France
- Lindeberg, M. & Hjort, K. (2003). Interconnected nanowire clusters in polyimide for flexible circuits and magnetic sensing applications, *Sensors and Actuators A*, Vol. 105, No. 2, July 2003, 150-161, 0924-4247
- Masuda, H. & Fukuda, K. (1995). Ordered metal nanohole arrays made by a 2-step replication of honeycomb structures of anodic alumina, *Science*, Vol. 268, No. 5216, June 1995, 1466-1468, 0036-8075
- Mayergoyz, I.D. (1985). Hysteresis models from the mathematical and control-theory points of view, *Journal of Applied Physics*, Vol. 57, No. 8, August 1985, 3803-3805, 0021-8979
- Nielsh, K.; Müller, F.; Li, A-P. & Gösele, U. (2000). Uniform nickel deposition into ordered alumina pores by pulsed electrodeposition, *Advanced Materials*, Vol. 12, No. 8, April 2000, 582-586, 0935-9648
- O'Sullivan, J.P. & Wood, G.C. (1970). Morphology and mechanism of formation of porous anodic films on aluminum, *Proceedings of the Royal Society of London, serie A*, Vol. 317, No. 1731, July 1970, 511-543, 1471-2954
- Peixoto, T.R.F. & Cornejo, D.R. (2008). Characterizing magnetic interactions in Ni nanowires by FORC analysis, *Journal of Magnetism and Magnetic Materials*, Vol. 320, No. 14, July 2008, E279-E282, 0304-8853
- Piroux, L.; Renard, K.; Guillemet, R.; Mátéfi-Tempfli, S.; Mátéfi-Tempfli, M.; Antohe, V.A.; Fusil, S.; Bouzehouane, K. & Cros, V. (2007). Template-grown NiFe/Cu/NiFe nanowires for spin transfer devices, *Nano Letters*, Vol. 7, Septembre 2007, 2563-2567, 1530-6984
- Piroux, L.; George, J.M.; Despres, J.F.; Leroy, C.; Ferain, E.; Legras, R.; Ounadjela, K. & Fert, A. (1994). Giant magnetoresistance in magnetic multilayered nanowires, *Applied Physics Letters*, Vol. 65, No. 19, November 1994, 2484-2486, 0003-6951
- Pirota, K.R.; Navas, D.; Hernandez-Velez, M.; Nielsch, K. & Vazquez, M. (2004). Novel magnetic materials prepared by electrodeposition techniques: arrays of nanowires and multi-layered microwires, *Journal of Alloys and Compounds*, Vol. 369, No. 1-2, April 2004, 18-26,
- Preisach, F. (1938). Über die magnetische Nachwirkung. *Zeitschrift für Physik*, Vol. 94, 1938, 277-302, 0722-3277. A presentation of the classical Preisach model is accessible in section 1.1 of Mayergoyz, I. (2003). *Mathematical models of hysteresis and their applications*, Elsevier, 978-0124808737, New York, USA
- Ross C.A. (2001). Patterned magnetic recording media, *Annual Review of Materials Research*, Vol. 31, 2001, 203-235, 1531-7331
- Saib, A.; Darques, M.L.; Piroux, L.; Vanhoenacker-Janvier, D. & Huynen, I. (2005). An Unbiased Integrated Microstrip Circulator Based on Magnetic Nanowired Substrate, *IEEE Transactions on Microwave Theory and Techniques*, Vol. 53, No. 6, June 2005, 2043-2049, 0018-9480
- Saib, A.; Vanhoenacker-Janvier, D.; Raskin, J.-P.; Crahay, A. & Huynen, I. (2001). Microwave tunable filters and nonreciprocal devices using magnetic nanowires, *Proceedings of the 2001 1st IEEE Conference on Nanotechnology (IEEE-NANO 2001)*, pp. 260-265, 0-7803-7215-8, Maui, USA, October 2001, IEEE, Piscataway, USA

- Spinu, L.; Stancu, A.; Radu, C.; Li, F. & Wiley, J.B. (2004). Method for magnetic characterization of nanowire structures, *IEEE Transactions on Magnetics*, Vol. 40, No. 4, July 2004, 2116-2118, 0018-9464
- Stoner, E.C. & Wohlfarth, E.P. (1948). A mechanism of magnetic hysteresis in heterogeneous alloys, *Philosophical Transactions of the Royal Society of London*, Vol. A240, 1948, 599-642, 0080-4649. Reprinted in *IEEE Transactions on Magnetics*, Vol. 27, No. 4, July 1991, 3475-3518, 0018-9464
- Tang, X.T.; Wang, G.C. & Shima, M. (2007). Magnetic layer thickness dependence of magnetization reversal in electrodeposited CoNi/Cu multilayer nanowires, *Journal of Magnetism and Magnetic Materials*, Vol. 309, No. 2, February 2007, 188-196, 0304-8853
- Thurn-Albrecht, T.; Schotter, J.; Kästle, C.A.; Emley, N.; Shibauchi, T.; Krusin-Elbaum, L.; Guarini, K.; Black, C.T.; Tuominen, M.T. & Russell, T.P. (2000). Ultrahigh-density nanowire arrays grown in self-assembled diblock copolymer templates, *Science*, Vol. 290, No. 5499, December 2000, 2126-2129, 0036-8075
- Wernsdorfer, W.; Doudin, B.; Maily, D.; Hasselbach, K.; Benoit, A.; Meier, J.; Ansermet, J.-P. & Barbara, B. (1996). Nucleation of magnetization reversal in individual nanosized nickel wires, *Physical Review Letters*, Vol. 77, No. 9, August 1996, 1873-1876, 0031-9007
- Ye, B.; Li, F.; Cimpoesu, D.; Wiley, J.B.; Jung, J.-S.; Stancu, A. & Spinu, L. (2007). Passive high-frequency devices based on superlattice ferromagnetic nanowires, *Journal of Magnetism and Magnetic Materials*, Vol. 316, No. 2, September 2007, E56-E58, 0304-8853
- Zhao, S.; Chan, K.; Yelon, A. & Veres, T. (2007). Preparation of open-through anodized aluminium oxide films with a clean method, *Nanotechnology*, Vol. 18, No. 24, June 2007, 245304, 0957-4484

IntechOpen



## **Electrodeposited Nanowires and their Applications**

Edited by Nicoleta Lupu

ISBN 978-953-7619-88-6

Hard cover, 228 pages

**Publisher** InTech

**Published online** 01, February, 2010

**Published in print edition** February, 2010

The book offers a new and complex perspective on the fabrication and use of electrodeposited nanowires for the design of efficient and competitive applications. While not pretending to be comprehensive, the book is addressing not only to researchers specialized in this field, but also to Ph.D. students, postdocs and experienced technical professionals.

### **How to reference**

In order to correctly reference this scholarly work, feel free to copy and paste the following:

Fanny Béron, Louis-Philippe Carignan, David Ménard and Arthur Yelon (2010). Extracting Individual Properties from Global Behaviour: First-order Reversal Curve Method Applied to Magnetic Nanowire Arrays, Electrodeposited Nanowires and their Applications, Nicoleta Lupu (Ed.), ISBN: 978-953-7619-88-6, InTech, Available from: <http://www.intechopen.com/books/electrodeposited-nanowires-and-their-applications/extracting-individual-properties-from-global-behaviour-first-order-reversal-curve-method-applied-to->

**INTECH**  
open science | open minds

### **InTech Europe**

University Campus STeP Ri  
Slavka Krautzeka 83/A  
51000 Rijeka, Croatia  
Phone: +385 (51) 770 447  
Fax: +385 (51) 686 166  
[www.intechopen.com](http://www.intechopen.com)

### **InTech China**

Unit 405, Office Block, Hotel Equatorial Shanghai  
No.65, Yan An Road (West), Shanghai, 200040, China  
中国上海市延安西路65号上海国际贵都大饭店办公楼405单元  
Phone: +86-21-62489820  
Fax: +86-21-62489821

© 2010 The Author(s). Licensee IntechOpen. This chapter is distributed under the terms of the [Creative Commons Attribution-NonCommercial-ShareAlike-3.0 License](https://creativecommons.org/licenses/by-nc-sa/3.0/), which permits use, distribution and reproduction for non-commercial purposes, provided the original is properly cited and derivative works building on this content are distributed under the same license.

IntechOpen

IntechOpen